

We are IntechOpen, the world's leading publisher of Open Access books Built by scientists, for scientists

5,300

Open access books available

130,000

International authors and editors

155M

Downloads

Our authors are among the

154

Countries delivered to

TOP 1%

most cited scientists

12.2%

Contributors from top 500 universities



WEB OF SCIENCE™

Selection of our books indexed in the Book Citation Index
in Web of Science™ Core Collection (BKCI)

Interested in publishing with us?
Contact book.department@intechopen.com

Numbers displayed above are based on latest data collected.

For more information visit www.intechopen.com



The Hintze Ribeiro Bridge Collapse and the Lessons Learned

José Simão Antunes Do Carmo

Abstract

In March 2001, a serious accident occurred in Portugal during a flood on the Douro River, next to Porto, Portugal. The collapse of the Hintze Ribeiro Bridge killed 59 people traveling in a bus and in three cars that fell into the Douro River. This bridge was built at the end of the 19th century on a curve of the Douro River, next to the mouth of the Tâmega River, approximately 50 km upstream of Porto. It was found that the combined effects of sand dredging in the 25 years prior to the accident (1975–2000) and the erosion produced by five consecutive floods between December 2000 and March 2001 were the main causes of this accident. Aiming to contribute to the prevention of occurrences such as that registered in Portugal with the collapse of the Hintze Ribeiro Bridge, a brief overview of this bridge is presented herein, as well as the causes that led to the collapse, some reflections on the processes involved, and, mainly, the lessons learned.

Keywords: Douro River, bridge collapse, floods, sediment transport, computational model, numerical simulations

1. Introduction

In March 2001, the collapse of the Hintze Ribeiro Bridge killed 59 people that were crossing the bridge at the Douro River [1] in a bus and three cars. The bridge collapse occurred on the night of 4 March 2001 when the Douro River flooded. The accident happened after the fifth river flood in a series of flood waves that started on 6th December 2000, all with peaks greater than 8000 m³/s.

This bridge was built at the end of the 19th century over a curve of the Douro River, near the mouth of the Tâmega River. In the 1980s, a dam was built downstream (Crestuma–Lever), whose reservoir reached the bridge and began affecting its pillars. Upstream of the section where the Hintze Ribeiro Bridge was located are Carrapatelo Dam on the Douro River and Torrão Dam on the Tâmega River (**Figure 1**).

2. Background

The Hintze Ribeiro Bridge, also known as the Entre-os-Rios Bridge, was built over the Douro River between 1884 and 1886 to link the village of Entre-os-Rios to Castelo de Paiva. The bridge structure consisted of six pillars, with only two permanently exposed to the flow (pillars P2 and P3), while P4 and P5 were implanted



Figure 1.
An actual perspective of the entre-os-Rios village. The second bridge seen in this perspective did not exist in 2001. The Hintze Ribeiro bridge was located in the same section as the first bridge (the nearest) seen in this image (adapted from [2]).

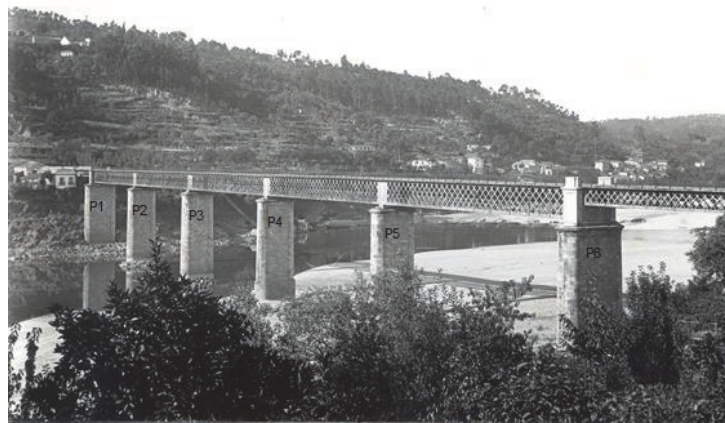


Figure 2.
Photo of the Hintze Ribeiro bridge, dated 1931 [3, 4].

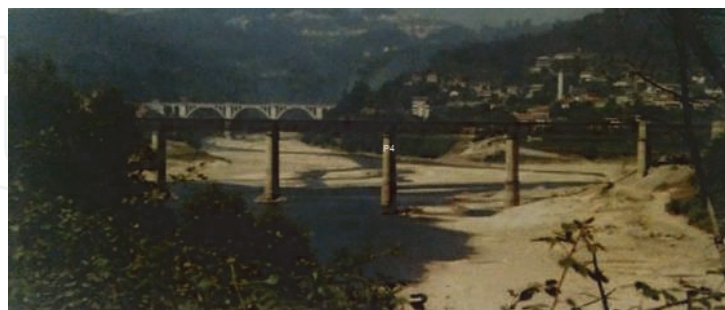


Figure 3.
Photo of the Hintze Ribeiro bridge taken in the late 1970s before the construction of Crestuma-lever dam [5]. As in Figure 2, designations P1 to P6 were used for the pillars of the bridge starting from the right bank (in the figure, from left to right).

on a sand deposit that existed until 1975, as shown in **Figure 2** [3, 4]. In addition, looking at **Figure 2**, it can be seen that P2 and P3 were protected by rockfill. The P3 protection is seen more clearly in **Figure 3**.

The analysis carried out on the various river bathymetric surveys that took place from the beginning of the 20th century until the 1970s allowed us to conclude that there were no bathymetric depressions along the stretch of the Douro River

upstream of the Hintze Ribeiro Bridge. With the increase in sand extraction from the 1970s onward, the sand deposit around P4 and P5 pillars (**Figure 2**) began decreasing due to direct extraction, having almost disappeared by 1982, as reported in a survey carried out in that year. This is also clearly shown in **Figure 3**.

Between the 1970s and the construction of the Crestuma–Lever reservoir in 1980s, large amounts of sand were extracted directly from the sand deposit at the left river bank where the bridge was located, and, after filling the reservoir, sand extraction continued across the entire reservoir by means of boats and by dredging the riverbed of the Douro River along the stretch upstream of the bridge. In **Figure 3**, a photo of the Hintze Ribeiro Bridge taken in the late 1970s before the construction of Crestuma–Lever Dam, one can observe the sand deposit irregularity, the almost inexistence of sand around P4, and the absence of rockfill protecting this pillar.

The sand extractions carried out upstream of the bridge, up to 7 km, created large riverbed depressions that retained part of the transported sands, which were already visible in the river bathymetry (outline) shown in **Figure 4**. Thus, the sandbar that naturally formed on the Douro River curve where the Hintze Ribeiro Bridge was located was never rebuilt.

By analyzing the technical documentation regarding the surveys of the bridge along the time (unpublished reports), it is possible to observe a lowering of the river bottom, next to P4, of approximately 11.5 m in the period from 1913 to 1982, and of 1.5 m between 1982 and 1989 [3]. Considering that the inner margin of the Douro River curve where P4 was implanted is a natural deposition area (see **Figures 1** and **2**), the lowering of the bottom level does not reflect this natural tendency.

The flows occurring in the section of the Douro River under the Hintze Ribeiro Bridge can be quantified by adding the flows released by the Carrapatelo and Torrão dams and the flows from the intermediate basins, resulting in the flow values discharged into the Cestuma–Lever reservoir, as shown in **Figure 5**. This figure shows the hourly average flows released from the Carrapatelo and Torrão dams, as well as the instantaneous flows measured at the entrance to the Crestuma–Lever reservoir.

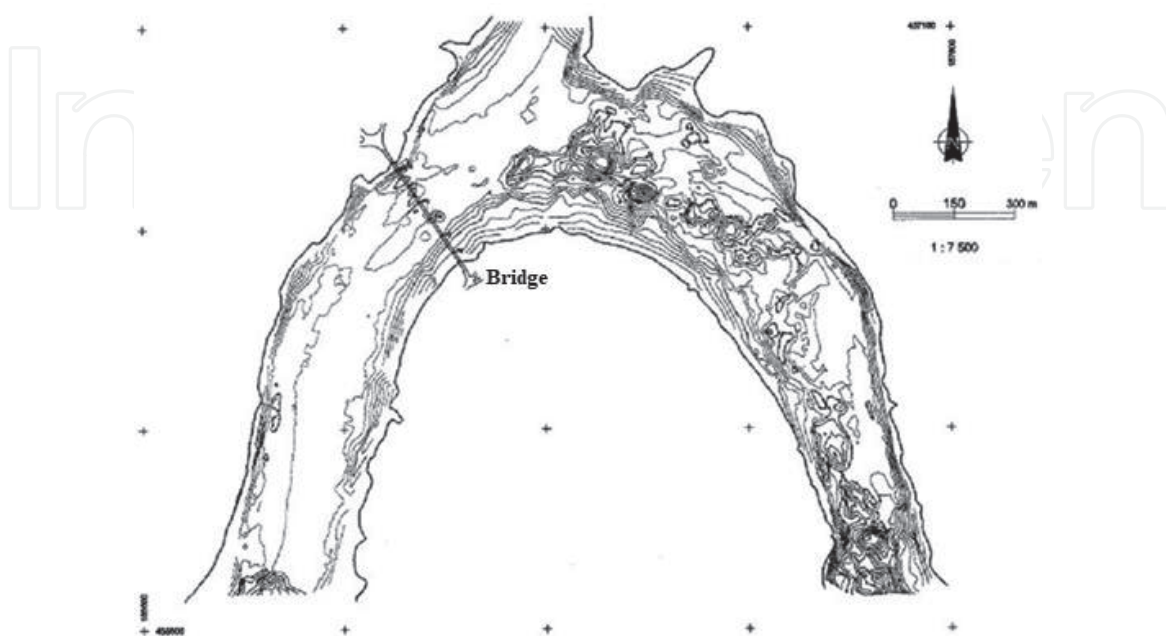


Figure 4. Douro River survey in entre-os-Rios carried out in 1982 [3]. The depressions are outlined upstream of the bridge, mostly along the thalweg.

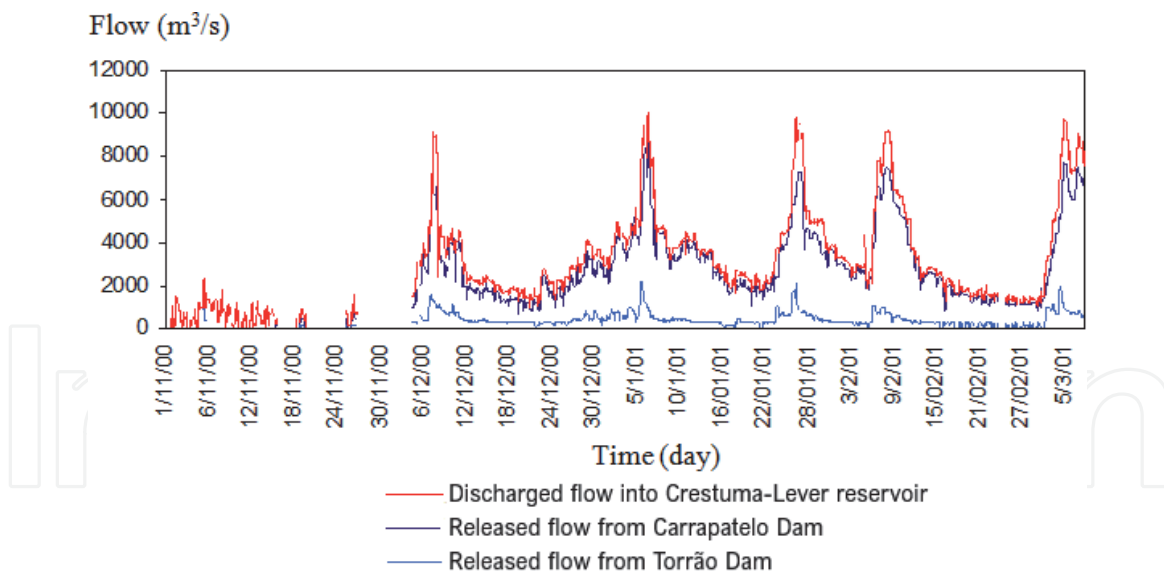


Figure 5. Released flows from the Carrapatelo and Torrão dams and the flow discharged into the Crestuma-lever reservoir between 1 November 2000 and 7 march 2001 [3, 4].

This sequence of five intense floods, with river flows that remained above 2000 m³/s for over three months, did not allow sufficient sediment deposition to guarantee the replacement of the previous bed conditions (former topography). In fact, in addition to generalized erosion of the river bed, these hydrodynamic conditions favor erosion around the foundations of structures (scour), as occurs for higher flows—in this case, approximately 2500 m³/s, estimated from the knowledge of the particle size of the bottom material and the critical velocity for the beginning of sediment transport by entrainment. The duration of the average daily flows of these floods are shown in **Table 1** [6].

Thus, the riverbed lowering of the order of 4 m, on average, observed between 2000 and 2001 in the stretch of the Douro River where the Hintze Ribeiro Bridge was located was mainly due to the five major floods observed from November 2000 to March 2001. As the amount of sand transported was not enough to meet the needs generated by the five floods, due to the retention of sand in the depressions that were created upstream by dredging or extracting sand over more than two decades, it was not possible to restore the conditions prior to the floods.

A video made by a specialized company in 1986 and, subsequently, a geological survey carried out in September 1988 allowed the detection of some corrosion in the metallic protections of P2 and P3, as well as the lack of riprap protecting P4 (**Figure 2**). In addition, even in 1986, a marked decrease in the level of the river bottom was also detected, especially near P4. It was discovered that the sand was at level – 2.40 m (approximately 38 m below the bridge deck).

Floods	Number of consecutive days with average daily flows released from Carrapatelo Dam equal or greater than 3000 m ³ /s
1 December 2000 until 4 March 2001	2 days (7 and 8 December 2000) 2 days (10 and 11 December 2000) 14 days (2–15 January 2001) 8 days (25 January–1 February 2001) 6 days (7–12 February 2001) 2 days (3 and 4 March 2001)

Table 1. Average daily flow duration from 1 December 2000 to 4 march 2001 [6].

The survey carried out in 1988 showed that, in the case of the foundation of P4, the top of the metal campanula used for the excavation was located 43–44 m below the bridge deck, and the level of the river bottom was approximately 45.8 m below. This topo-hydrographic survey also made it possible to verify that the pillars were not supported on rock, but on alluvial soil.

In addition, analyzing the 1988 survey, it was also possible to conclude that at that time, there were approximately 9 m of sand above the foundation of P4. A new topo-hydrographic survey carried out 10 years later, in 1998, showed that the situation had worsened, as the bottom of the river lowered by approximately 1 m in the period 1988–1998.

As evidenced by the photo shown in **Figure 6**, taken a few days after the collapse of the bridge, P4 fell against the current and, therefore, against the effect of the natural flow, whose strength and resulting momentum would have pointed in exactly the opposite direction. Such behavior can only be explained by infra-excavation (scour), which was the dominant process in the foundation of P4, putting it out of service. In fact, the location and magnitude of the scour hole usually occurs in front and around of the structure [3, 4].

The Hintze Ribeiro Bridge, although old, had a construction design and several elements that would have allowed a sufficient characterization of its stability. The surveys carried out made it possible to draw conclusions about the type of existing foundations and the state they were in (i.e., the video and a report made by a company specialized in underwater inspection in 1986, and the surveys carried out in 1988 and 1998). There were also technical memories with very detailed information about the bridge characteristics and construction conditions [7].

In the photo of the Hintze Ribeiro Bridge shown in **Figure 2**, dated 1931, the geometry and shape of the cross-section of the riverbed are clearly represented. P2 and P3 would have been the most affected by the flow of the river. It is also clear that protection of P2 and P3 already existed in 1931, as well as the sandbank on the inner edge of the curve where the bridge was located. **Figure 2** also shows that P4 was based on the sandbank, with a level of sand identical to that of P5.

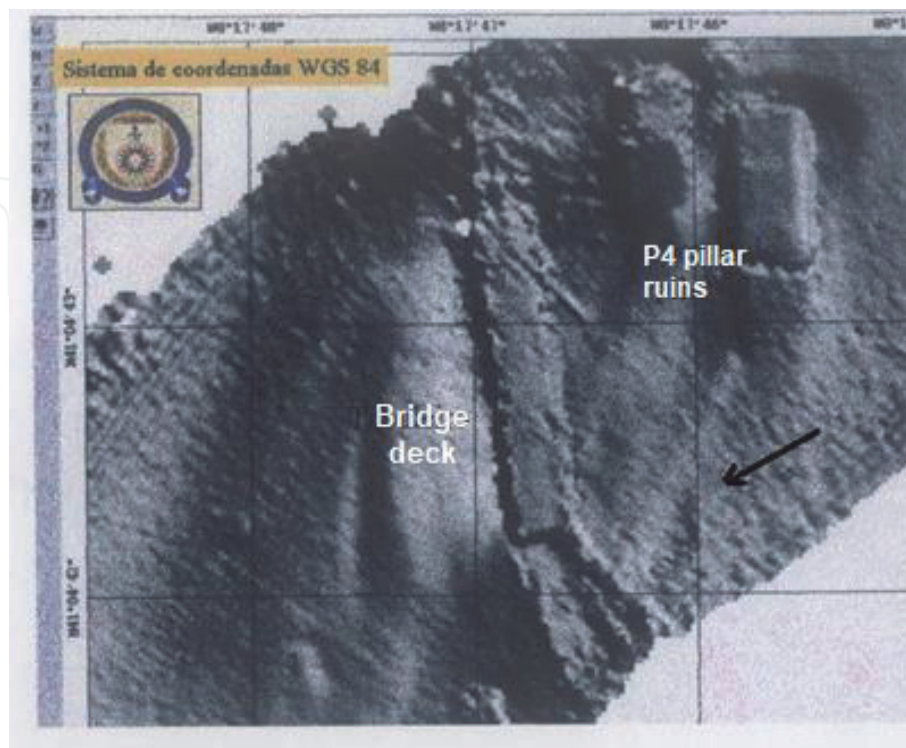


Figure 6.
Final position of the pillar 4 (P4), after the bridge collapse. The arrow indicates the direction of the flow [3, 4].

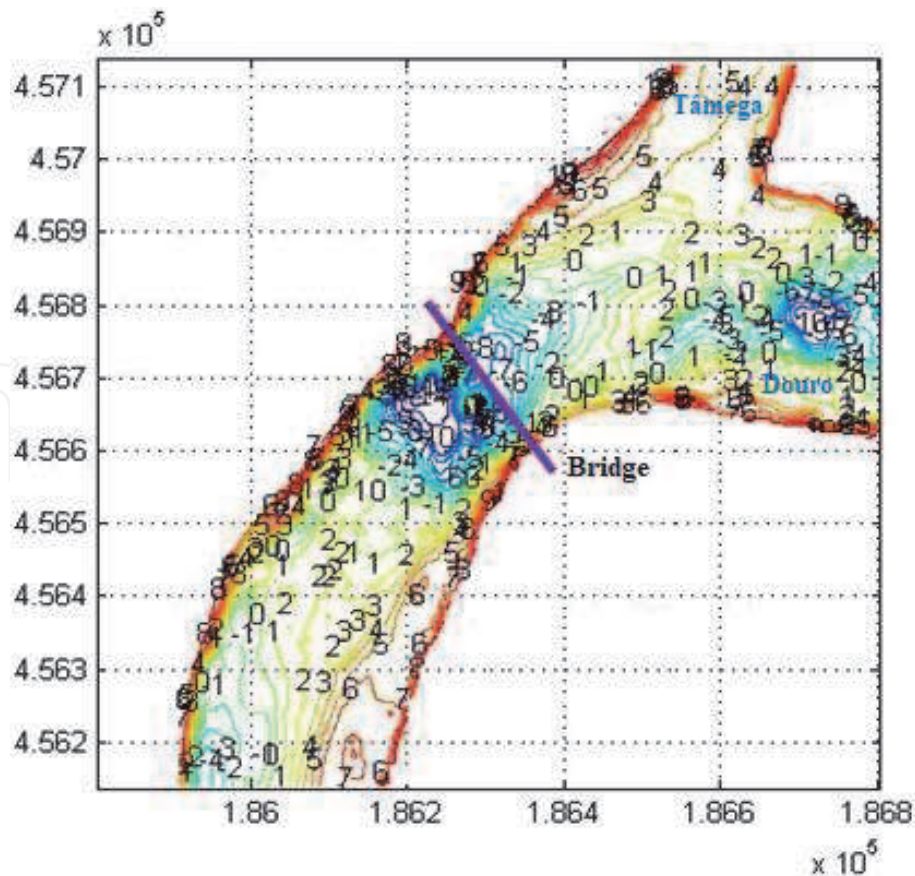


Figure 7. Douro River survey at entre-os-Rios carried out in 2002. The bluish lines with negative topographic dimensions identify the large existing depressions.

The large volume of sand extracted near the bridge, mainly from the mid-1970s until the construction of Crestuma–Lever Dam and, from there, along the entire length of the reservoir, mainly at various points upstream of the bridge, led to the destruction of the natural sand deposit that existed on the inner bank of the river curve. In addition, the large amounts of extracted sand and the lack of a natural sand supply led to the general lowering of the river bottom and the creation of many depressions along the river, especially in the area where the bridge was located, as documented in **Figure 7**.

The debasement of approximately 13.0 m detected in the period from the mid-1970s to 1989 was mainly due to sand extraction, as this stretch of the Douro River is an area of natural deposition, as evidenced by the photo dated 1931 shown in **Figure 2**.

3. The causes of the bridge collapse

3.1 Hydrodynamic causes

By reason of the successive and intense rains recorded in the period between 1 November 2000 and 7 March 2001, the average daily flow of the Douro River remained high for long periods of time, even exceeding the values recorded in previous historical floods. It was also found that the river flow remained very high from 4 March to at least 7 March 2001. Moreover, it is known that floods in alluvial beds, such as the Douro River where the Crestuma–Lever reservoir is located, cause changes in the bottom levels, although only temporary.

From December 2000 to March 2001, the main downgrade may have been caused by high floods (**Figure 5**). However, as this cause was not the only one, it is important to assess whether the bed levels at the beginning of the persistent floods were equivalent to those that existed in previous and equally intense floods, such as those of January 1996 (14 consecutive days), December 1989 (two floods lasting three and four days, respectively), and February 1979 (two floods lasting eight and six days, respectively). If differences can in fact be observed, the total drawdowns (and not just those related to each individual flood), would not have been the same and, as such, the last flood should not be considered as the only decisive factor of the river bottom degradation.

To compute the distribution of the velocity modules to which the P2, P3, P4, and P5 would have been subjected from 5 December 2000 to 4 March 2001, a two-dimensional morphodynamic model (*morphodyn*) in the horizontal plane (2DH) was used [4, 8]. The hydrodynamic module of this computational model solves the Saint-Venant equations, or shallow water equations, which can be deduced by vertically integrating the fundamental equations of fluid mechanics applied to a three-dimensional flow. Fluid incompressibility and hydrostatic pressure are assumed. These equations are written in the following conservative form [4, 8]:

$$\begin{aligned}\frac{\partial H}{\partial t} + \frac{\partial U}{\partial x} + \frac{\partial V}{\partial y} &= 0 \\ \frac{\partial U}{\partial t} + \frac{\partial F}{\partial x} + \frac{\partial G}{\partial y} &= E_x \\ \frac{\partial V}{\partial t} + \frac{\partial G}{\partial x} + \frac{\partial S}{\partial y} &= E_y\end{aligned}\quad (1)$$

In the system of Eq. (1), all variables are functions of x , y , and t . With $H = h$, the unknowns U , V , F , G , and S are written as $U = hu$, $V = hv$, $F = u^2h + \frac{1}{2}gh^2$, $G = uvh$, and $S = v^2h + \frac{1}{2}gh^2$, where h is the water depth, (u, v) are the depth averaged flow velocity components, and g is the acceleration due to gravity. The terms E_x and E_y in the second and third equations are written:

$$E_x(x, y, t) = -gH \frac{\partial \xi}{\partial x} + fV - \frac{1}{\rho} \tau_{fx} + \frac{\partial}{\partial x} \left(\varepsilon \frac{\partial U}{\partial x} \right) + \frac{\partial}{\partial y} \left(\varepsilon \frac{\partial U}{\partial y} \right) \quad (2)$$

$$E_y(x, y, t) = -gH \frac{\partial \xi}{\partial y} - fU - \frac{1}{\rho} \tau_{fy} + \frac{\partial}{\partial x} \left(\varepsilon \frac{\partial V}{\partial x} \right) + \frac{\partial}{\partial y} \left(\varepsilon \frac{\partial V}{\partial y} \right) \quad (3)$$

In Eqs. (2) and (3), ξ means bed levels, ε is the turbulent diffusion coefficient, and f is the Coriolis parameter, given by $2\Omega \sin(\phi)$, where ϕ is the latitude and Ω is the angular velocity of the Earth about its axis, given by $\Omega = \frac{2\pi}{86160} s^{-1}$. The bed shear stresses are computed by the Manning–Strickler formula, which are given by:

$$\frac{\tau_{fx}}{\rho} = \frac{g(u^2 + v^2)^{1/2} u}{K^2 h^{7/3}} \quad \frac{\tau_{fy}}{\rho} = \frac{g(u^2 + v^2)^{1/2} v}{K^2 h^{7/3}} \quad (4)$$

In Eq. (4), $K = 1/n_s$ represents Manning's roughness coefficient. In terms of the equivalent sand grain diameter, n_s is given by $n_s = k_s^{1/6}/21.1$, $k_s \approx 2.5d_{50}$.

The system formed by Eqs. (1) is solved numerically using an explicit finite difference method based on the MacCormack's time-splitting scheme [9–11]. In order to apply this method, the Saint-Venant Eqs. (1) are split into two systems of

three equations throughout the Ox and Oy directions. The corresponding operators, L_x and L_y , take the following forms (5) and (6):

Operator L_x

$$\begin{aligned} \frac{\partial H}{\partial t} + \frac{\partial U}{\partial x} &= 0 \\ \frac{\partial U}{\partial t} + \frac{\partial F}{\partial x} &= -gH \frac{\partial \xi}{\partial x} - \frac{\tau_{fx}}{\rho} + fV + \frac{\partial}{\partial x} \left(\varepsilon \frac{\partial U}{\partial x} \right) \\ \frac{\partial V}{\partial t} + \frac{\partial G}{\partial x} &= \frac{\partial}{\partial x} \left(\varepsilon \frac{\partial V}{\partial x} \right) \end{aligned} \quad (5)$$

Operator L_y

$$\begin{aligned} \frac{\partial H}{\partial t} + \frac{\partial V}{\partial y} &= 0 \\ \frac{\partial U}{\partial t} + \frac{\partial G}{\partial y} &= \frac{\partial}{\partial y} \left(\varepsilon \frac{\partial U}{\partial y} \right) \\ \frac{\partial V}{\partial t} + \frac{\partial S}{\partial y} &= -gH \frac{\partial \xi}{\partial y} - \frac{\tau_{fy}}{\rho} - fU + \frac{\partial}{\partial y} \left(\varepsilon \frac{\partial V}{\partial y} \right) \end{aligned} \quad (6)$$

Considering the generic variable Q, the solution at time $(n + 1)\Delta t$ for the computational point (i, j) , is obtained through the following symmetric application (4, 8):

$$Q^{n+1} = L_x \left(\frac{\Delta t}{2} \right) L_y \left(\frac{\Delta t}{2} \right) L_y \left(\frac{\Delta t}{2} \right) L_x \left(\frac{\Delta t}{2} \right) Q^n \quad (7)$$

where each operator, L_x e L_y , is composed of a predictor–corrector sequence and n represents a generic time t . In the four predictor–corrector sequences of application (7), alternatively backward and forward space differences are used. The derivative discretization is performed as follows [4, 8]:

First operator L_x : Predictor–backward differences

Corrector–forward differences

First operator L_y : Predictor–backward differences

Corrector–forward differences

Second operator L_y : Predictor–forward differences

Corrector–backward differences

Second operator L_x : Predictor–forward differences

Corrector–backward differences

For the analysis, four hypotheses of initial conditions were considered: Bathymetry of the year 1982, with and without the sand deposit, and the year 2000, with and without the large depressions caused by the dredging that occurred upstream and downstream of the bridge. As the boundary conditions, the discharge flows of the Torrão and Carrapatelo dams were considered, plus 6% of the Carrapatelo flows, for taking into account the intermediate flows of the basin, namely, those of

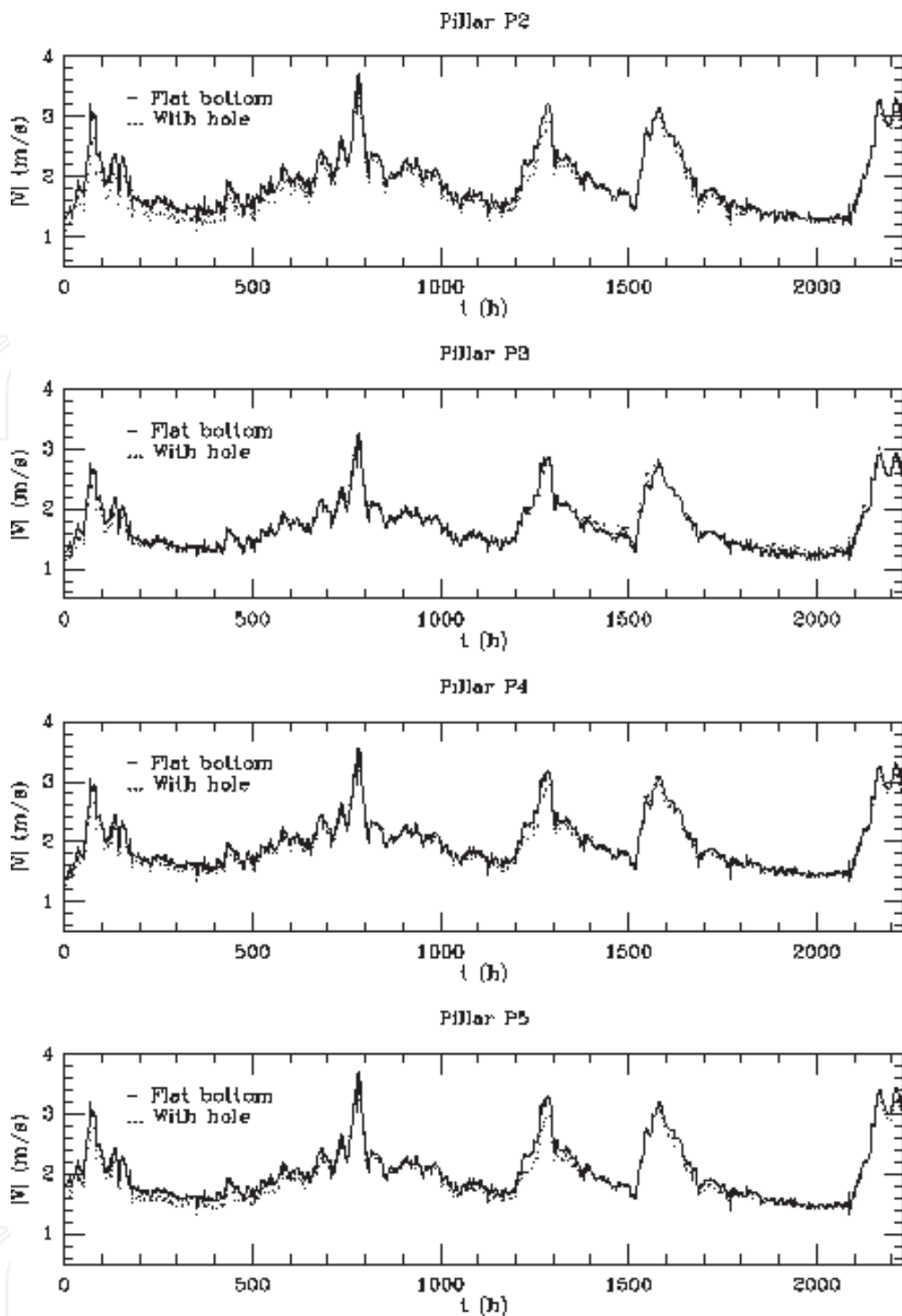


Figure 8.
Velocity module distributions, over time, near P2, P3, P4, and P5, in the period of 5 December 2000 to 4 March 2001.

the Paiva River basin. A grid with cell size of 25 m was used in each simulation. Considering a bathymetry of February 2000, with and without large depressions, the temporal distribution of the velocity modules, i.e., the vertically integrated average velocity, is presented in **Figure 8**, near the P2, P3, P4, and P5 from 5 December 2000 to 4 March 2001.

It is noticed that both P2 and P5 would have been subjected to the greater impacts, with an identical velocity module varying between 1.0 and 3.7 m/s.

Considering the four hypotheses related to the initial conditions, the use of the same model made it possible to estimate the velocity field that would have occurred approximately at the time of the accident (4 March 2001 at approximately 9:00 p.m.).

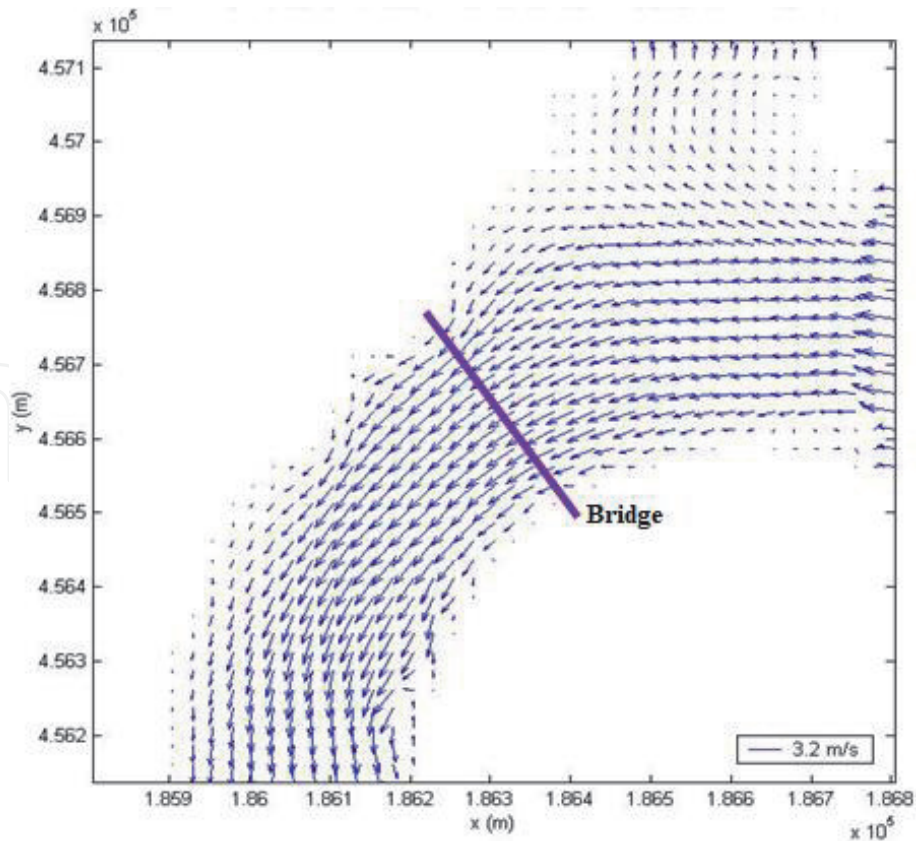


Figure 9. Velocity field obtained on 4 march 2001 at approximately 12:00 p.m., considering a bathymetry of 2000 without large depressions near the pillars. Note that the flow distribution is $10,000 \text{ m}^3/\text{s}$ at Carrapatelo dam and $2,000 \text{ m}^3/\text{s}$ at Torrão dam, therefore with a 5:1 ratio.

Initial Bathymetry	Pillar P2	Pillar P3	Pillar P4	Pillar P5
1982 without sand deposit	3.6	3.2	3.7	3.4
1982 with sand deposit	3.7	3.2	3.6	3.6
2000 without large depression	3.7	3.3	3.6	3.7
2000 with large depression	3.6	3.3	3.5	3.6

Table 2. Maximum flow velocities near P2–P5 that occurred during the floods from 5 December 2000 to 4 march 2001 (m/s).

Figure 9 shows one of these situations, which corresponds to the velocity field obtained on 4 March 2001 at approximately 12:00 p.m.

The changes in the river bottom observed in the four topographic surveys carried out in 1982, 1989, 2000, and 2001 led to some variations in the velocity values. However, these variations were not very significant, which is explained by the relationship between the changes in bottom levels, in the order of a few meters, and the high flow depths, in the order of 20 m for the flood peaks under analysis.

In contrast, when comparing the velocity fields obtained on 4 March 2001, considering the initial bathymetries (without and with large depressions), no significant differences are observed, although the riverbeds obtained corresponded to different evolutions in the analyzed period: 5 December 2000 to 4 March 2001 (**Figure 8**).

The differences in velocity in the simulations carried out, considering several initial bathymetries of the river, were easily perceived by comparing the evolution over time of the velocity modules near P2, P3, P4, and P5 for the period from 5

December 2000 to 4 March 2001. This analysis made it possible to construct the following **Table 2** with the maximum values of the velocity modules that occurred for the flood peak on 6 January 2001.

Analyzing **Table 2**, it can be concluded that the velocity differences were very small ($<10\%$) and, as such, cannot be considered significant as to their direct effects.

The existence of a large depression in the riverbed generally leads to a decrease in the depth averaged velocity in its vicinity, when compared to the average velocity outside of the depression. However, this behavior occurs simultaneously with changes in the velocity profile, especially close to the edges of the depression, leading to changes in the turbulence pattern.

In the Douro River area, with large floods in a curved stretch and where very strong secondary currents occur, the pattern of turbulence is already very complex, even without large depressions. Although it is not possible to identify in detail the full complexity of the turbulence generated by dredging, it can be said that, although mild, there may have been an increase in turbulence.

In addition, the rockfill around the foundations of P2 and P3 had little effect on the mean flow velocity fields, as they resulted in a very small reduction in the cross-section. In fact, for a 4000 m^2 flood section, the riprap corresponded to just 140 m^2 , which is a reduction of approximately 3.5% . The errors resulting from the reduction in the flooded section were smaller than the errors made in determining the flood beds and would not have had a significant effect on the general pattern. Locally, the rockfill had a protective effect, as it would have reduced the scour process.

The river flows released by the Torrão and Carrapatelo dams are expected to have influenced the velocity field near the bridge. Indeed, the velocity field corresponding to a given total flow should have changed depending on whether the total flow was released only from Carrapatelo Dam, only from Torrão Dam, or in different quantities from each dam. When the major floods occurred, the most likely flow distributions would have been in the order of $10,000\text{ m}^3/\text{s}$ at Carrapatelo Dam, while at Torrão Dam, they would not have exceeded $2000\text{ m}^3/\text{s}$, keeping a 5:1 ratio. The numerical computation made it possible to verify that, in most cases, the flow from Torrão Dam was diverted by the flow from Carrapatelo Dam to the right bank of the river, as shown in **Figure 9**.

It should be noted that the discharge from Torrão Dam consists of clear waters, without the sediments that are trapped in the dam, while the floodwaters of the Douro River present high concentrations of sediments. It turns out that these waters would not have mixed immediately, since the flow from Torrão Dam passed close to the right bank of the river. In fact, less water turbidity was observed on this river bank. Thus, the direct influence of the flow from Torrão Dam on P4 was practically nil. It was also observed numerically that this influence was still insignificant for relations in the order of 40% of the flows from Torrão Dam, as happened during some hours in the winter flood of 2000–2001.

In the numerical computations made using the *morphodyn* model (described above), only some influence on P4 for the flows from the Torrão and Carrapatelo dams of the same order of magnitude was noticeable. This is shown in **Figures 10** and **11** for a relationship between the flows discharged by these dams of 0.50 (possible event, although unlikely) and 1.0 (a very rare event, only possible with careless management of the dams).

3.2 Morphodynamic causes

The topographic surveys made it possible to quantify the temporal evolution of the erosive processes in the riverbed of the Douro River, in the cross-section where

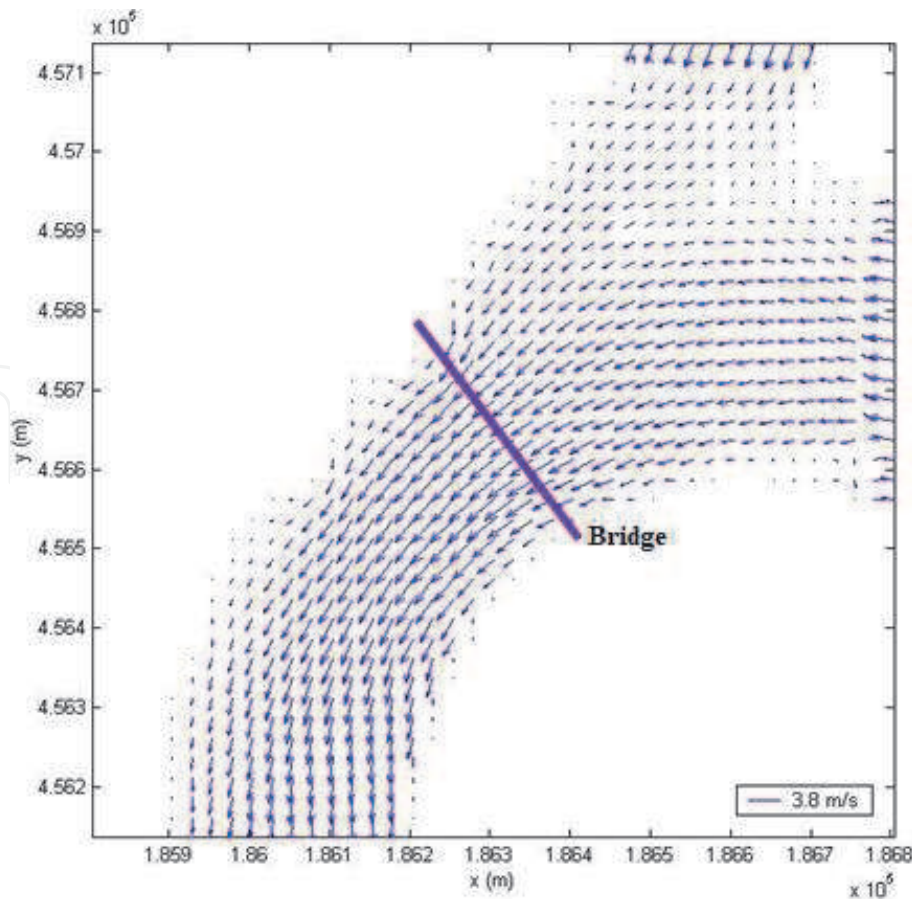


Figure 10. Velocity field obtained after three days of simulation, considering the bathymetry of the year 2000 without large depressions near the pillars and constant flows of $3000 \text{ m}^3/\text{s}$ in Torrão dam and $6000 \text{ m}^3/\text{s}$ in Carrapatelo dams.

the Hintze Ribeiro Bridge was located, and in the surrounding area. Furthermore, the theoretical analysis of erosive phenomena allowed us to obtain the following conclusions, from the most important to the least important:

1. The general erosion caused by the extraction of sand from the riverbed is an artificial process, which leaves deep scars, and was easily identified in the analyses performed. The comparison of topographic surveys carried out at different times, one before the extractions and the other after the extractions, allowed to quantify the volume differences resulting from the extractions. The sand depression that existed on the curve, clearly visible in old photos (**Figure 2**), as well as on old military maps, disappeared due to the sand extractions that were carried out more intensively from 1975. The large depressions caused by sand extractions were subsequently deformed and partially filled by the intense floods.
2. The scour process around the bridge pillars is partly temporary, with some residual erosion remaining during drought flows (on average).
3. The general erosion that occurs during flooding is temporary, with the previous level of the riverbed recovered some time later; in the Douro River case, it was recovered in weeks.
4. The general drawdown, or degradation, is caused by a tendency of decreasing the supply of sediment. In the Douro River case, this degradation may have

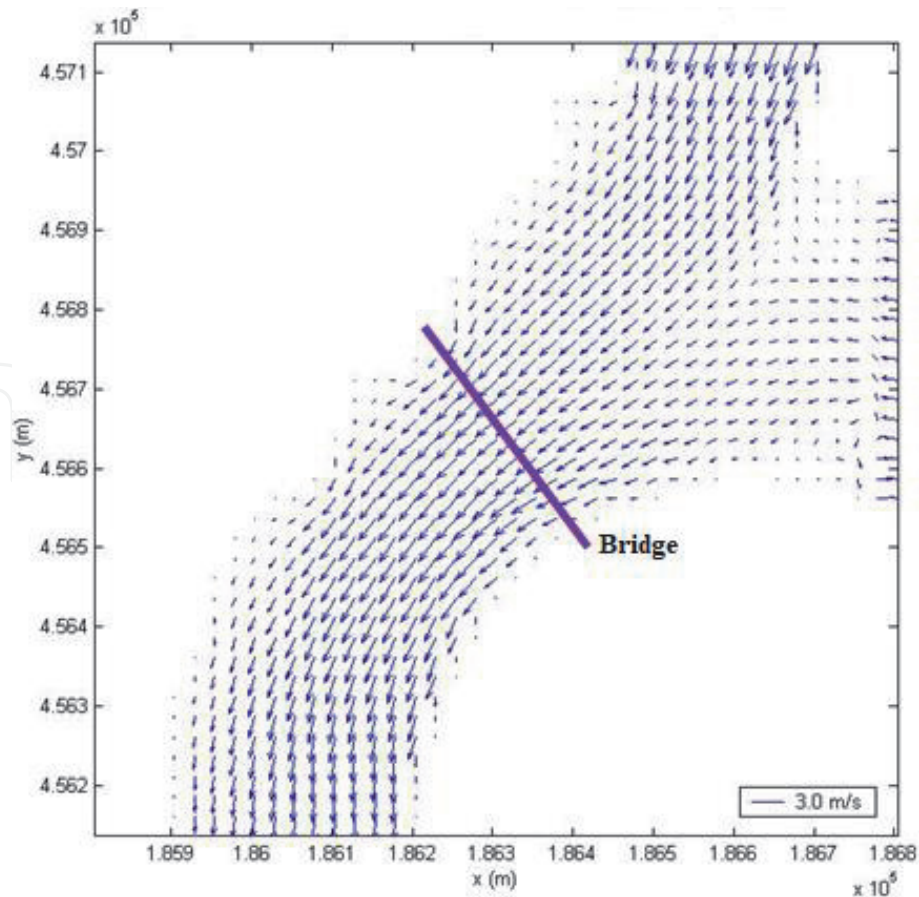


Figure 11. Velocity field obtained after three days of simulation, considering the bathymetry of the year 2000 without large depressions near the pillars and constant flows of $3000 \text{ m}^3/\text{s}$ in Torrão dam and $3000 \text{ m}^3/\text{s}$ in Carrapatelo dam.

increased due to the extraction of sand upstream from the bridge. The large depressions were, in general, fed upstream by the sediments that pass through Carrapatelo Dam, thus retaining the effects of erosion (degradation) downstream, which could be felt up to kilometers away.

The processes of natural erosion begin when the transport capacity of the runoff exceeds the critical stress necessary for the start and transport of sediments by dragging or in suspension. The critical velocity for the beginning of the movement of sandy material is, on the other hand, a function of the granulometry of this material. According to the particle size analysis data of the foundation of P4, the median diameter (d_{50}) of the sediment was in the range of 2–3 mm [3].

The particle size characterization of alluvial riverbeds requires a collection of samples that adequately covers the analyzed area. In this case, there were not enough samples to determine a characteristic value, but a set of values is enough to carry out analysis of sand transport along the river, given the usual errors in other parameters and variables.

According to several equations that appear in the literature, the critical velocity computation, or the initial velocity for the beginning of the movement of sand particles, leads to mean flow velocity values between 0.7 and 0.9 m/s. These critical velocities correspond to river flows between 2200 and $2600 \text{ m}^3/\text{s}$ [3].

The sediment transport phenomenon is a function of the river flow, the granulometry, and sediment shapes. Therefore, transport occurs at different velocities depending on the size of the particles. In the Douro River case, which may have relatively coarse particles at the bottom, sediment transport from the larger

particles, in the order of 6 cm, can occur at velocities above 1.80 m/s, while for the finer particles, around 0.50 mm, sediment transport can occur at velocities around 0.40 m/s [3]. As such, it can be stated that deposition will occur for different particle sizes during flood flows, starting with the coarse ones and ending with the thinner ones. For the coarse sediments, sediment transport can occur for relatively high flows, in the order of 3000 m³/s.

In the Carrapateiro reservoir, as well as in the reservoirs located upstream, the sediment retention is zero, as was proven by the topographic surveys of all of reservoirs in the Douro River carried out by the Portuguese IPTM (Instituto Português e dos Transportes Marítimos) in 2002 (unpublished report). Comparing the longitudinal profile of the Douro River after the great flood of 1962 and the longitudinal profile of 2002 highlighted that there was no silting up in the Douro River dams.

The Torrão Dam reservoir retains practically all of the sediments that arrive there, which was also easy to conclude by the clear color of the water discharged from the dam during the floods, that is, without sediment transport. However, the amount of sandy sediments transported by the Tâmega River is much lower than that transported by the Douro River. In the Douro Basin Hydrographic Plan, a contribution of 37,500 t/year from the Tâmega River is estimated, which corresponds to approximately 7.5% of the contribution from the Douro Basin, which is 500,000 t/year [3].

The decrease in sandy sediment in the Tâmega River is not enough to alter the alluvial behavior of the Douro River. This was confirmed by the topographic surveys carried out at the mouth of the Tâmega River, after the construction of the Torrão Dam, having at that time clarified the great dominance of the Douro River.

This same conclusion was confirmed by the use of the *morphodyn* model, which solved the following sediment conservation Eq. (8), together with the system of hydrodynamic Eqs. (1) (morphodynamic module). Neglecting the contribution of the local variations of sediment concentration [4, 8, 12], this equation is written as:

$$(1 - \lambda) \frac{\partial \xi}{\partial t} + \frac{\partial}{\partial x} \left[\langle q_b + q_s \rangle_x - \langle \varepsilon_b |q_b| + \varepsilon_s |q_s| \rangle_x \frac{\partial \xi}{\partial x} \right] + \frac{\partial}{\partial y} \left[\langle q_b + q_s \rangle_y - \langle \varepsilon_b |q_b| + \varepsilon_s |q_s| \rangle_y \frac{\partial \xi}{\partial y} \right] = \langle q_{sl} \rangle \quad (8)$$

where $\langle \dots \rangle$ represents the average quantities, λ is the sediment porosity, q_b and q_s [$m^3 s^{-1} / m.l.$] represent the bed load and suspended load, respectively, per unit width of the watercourse, and q_{sl} [$m^3 s^{-1} / m.l. / m.l.$] represents the input or output sediment transport, per unit width of the main watercourse and per unit width of the tributary.

Such as for solving the system of Eqs. (1), Eq. (8) is also split into the following operators:

Operator L_x

$$(1 - \lambda) \frac{\partial \xi}{\partial t} + \frac{\partial R}{\partial x} = \langle q_{sl} \rangle_x \quad (9)$$

Operator L_y

$$(1 - \lambda) \frac{\partial \xi}{\partial t} + \frac{\partial S}{\partial y} = \langle q_{sl} \rangle_y \quad (10)$$

where $R = \langle q_b + q_s \rangle_x - \langle \varepsilon_b |q_b| + \varepsilon_s |q_s| \rangle_x \frac{\partial \xi}{\partial x}$ and $S = \langle q_b + q_s \rangle_y - \langle \varepsilon_b |q_b| + \varepsilon_s |q_s| \rangle_y \frac{\partial \xi}{\partial y}$.

Such as in hydrodynamics, the solution at time $(n + 1)\Delta t$ for the computational point (i, j) , is also obtained through symmetric application (4, 8).

The sediments transported by entrainment (11) and in suspension (12) are written as [4, 8]:

$$\langle q_{b_x} \rangle = \frac{c_f}{g(s-1)} \frac{\varepsilon_b}{\tan\varphi} |u|^2 u \quad \langle q_{b_y} \rangle = \frac{c_f}{g(s-1)} \frac{\varepsilon_b}{\tan\varphi} |v|^2 v \quad (11)$$

$$\langle q_{s_x} \rangle = \frac{c_f}{g(s-1)} \frac{\varepsilon_s}{w_s} |u|^3 u \quad \langle q_{s_y} \rangle = \frac{c_f}{g(s-1)} \frac{\varepsilon_s}{w_s} |v|^3 v \quad (12)$$

where ε_b and ε_s are the efficiencies, with values in the intervals of $0.10 \leq \varepsilon_b \leq 0.30$ and $0.01 \leq \varepsilon_s \leq 0.03$, s is the sediment density ($s \approx 2.65$), φ is the internal angle of friction of the sediment, w_s represents the sediment fall velocity, and c_f is a current friction coefficient given by $c_f = \sqrt{0.5f_c}$, with the bed-roughness coefficient $f_c = 0.06 \left(\log_{10} \frac{12h}{k_s} \right)^{-2}$, $k_s \approx 2.5d_{50}$.

Figures 12 and 13 show the numerical evolution of the alluvial riverbed after a three-day simulation, due to the hydrodynamic action of the velocity fields shown in **Figures 10 and 11**, corresponding to the relationships of 0.5 and 1.0 between the flows discharged from Torrão Dam and Carrapatelo Dam, respectively. In these simulations, the initial bathymetry of February 2000 was used, which is basically the one shown in **Figure 7** without the large depressions near the pillars.

Thus, since the transport capacity of the Douro River is much higher than that of the Tâmega River, a decrease in the contribution of sediments from this basin does

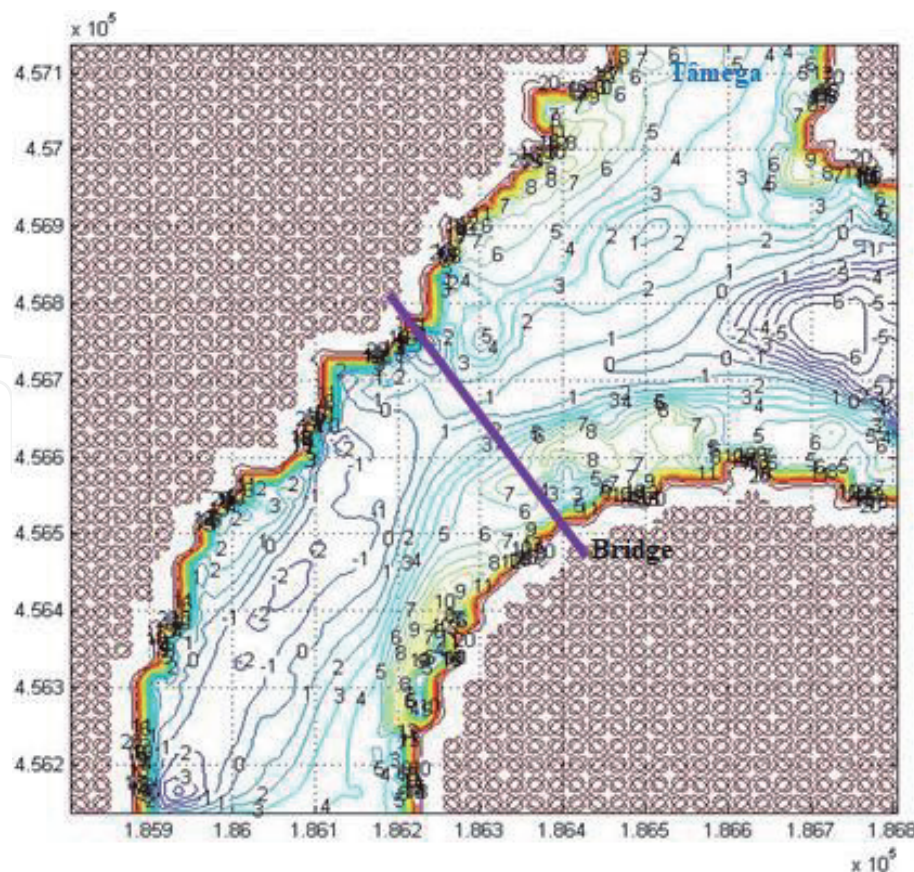


Figure 12. Riverbed configuration obtained after three days, considering an initial bathymetry of the year 2000 without large depressions near the pillars and constant flows of $3000 \text{ m}^3/\text{s}$ in Torrão dam and $6000 \text{ m}^3/\text{s}$ in Carrapatelo dam.

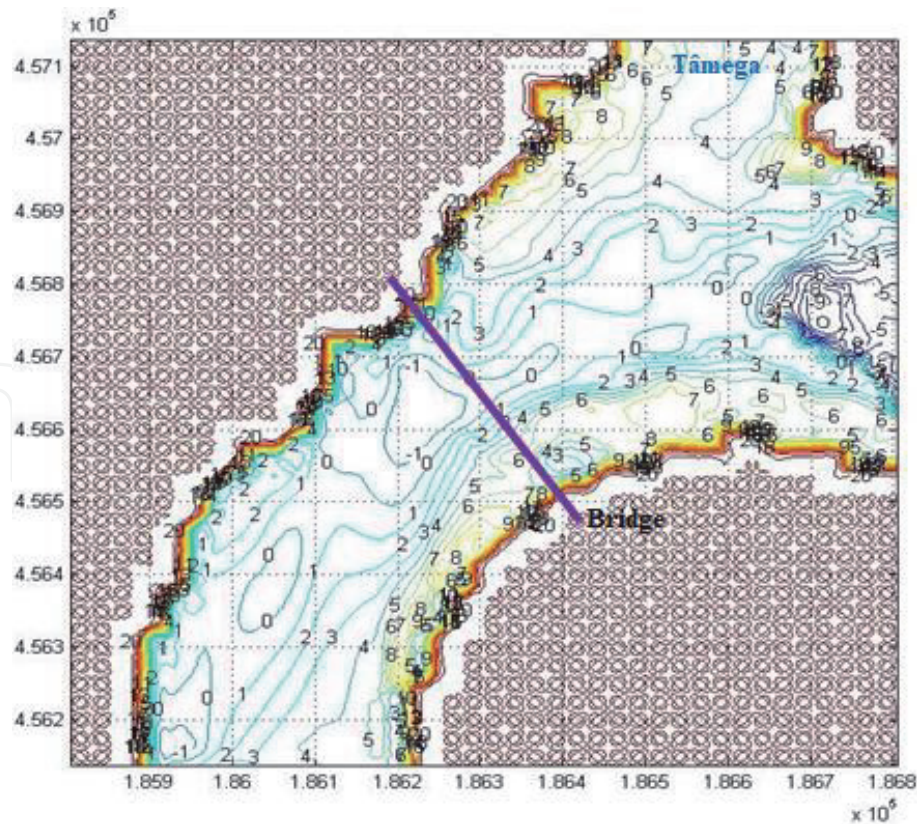


Figure 13. Riverbed configuration obtained after three days, considering an initial bathymetry of the year 2000 without large depressions near the pillars and constant flows of $3000 \text{ m}^3/\text{s}$ in Torrão dam and $3000 \text{ m}^3/\text{s}$ in Carrapatelo dam.

not manifest itself significantly in the general mobility of the alluvial bottom of the Douro River.

4. Discussion and conclusions

The analyses carried out on the various surveys performed since the beginning of the 20th century until the 1970s allowed us to conclude that there were no significant depressions along the stretch of the Douro River upstream of the Hintze Ribeiro Bridge.

Whenever the lowering of alluvial beds is quantified, there must be at least two plots considered: those related to the occurrence of floods (general temporary erosion) and those related to medium-term trends (degradation). The latter is a slower phenomenon, more difficult to reverse, and can have several causes when compared to the drawdowns during floods, namely, imbalances in the natural supply of sediments, upstream reservoir silting, upstream dredging, and riverbed lowering downstream.

Besides the general, slow and fast, and reversible and irreversible lowering, a localized debasement also occurred near P4, as well as close to the other bridge pillars, which were caused by the presence of rigid obstacles.

The large bathymetric depressions identified upstream and next to the bridge pillars, identified in the 1980s and 1990s, correspond to the sum of several causes, namely, the extraction of inert material, the general phenomenon of sediment transport (general erosion), and flow interaction with rigid obstacles, such as pillars (local erosion - scour). These depressions led to a reduction in the natural sediment transport downstream.

With the increase in sand extraction from the 1970s onward, the sand deposit at the left river bank decreased due to direct extraction, having almost disappeared in 1982, as shown in the survey carried out that year (see **Figures 3** and **4**).

Despite the natural complexity of a century-old bridge collapse, the analysis of safety conditions, and considering the hydrodynamic phenomena involved in the Hintze Ribeiro Bridge collapse, it is possible to draw some conclusions. As such, it can be said that:

- In 1931, P4 was implanted in a natural silting area.
- Both P2 and P3 were protected by rockfill before 1931.
- The riverbed lowering in the P4 area was mainly due to sand extraction, as it is a natural silting area.
- The sand levels above the foundation base, before the 2000–2001 floods, were between 7 and 8 m.
- Torrão Dam discharges did not influence the collapse of P4.
- The collapse of the bridge occurred after five consecutive intense floods, which caused P4 to fall due to local scour and general erosion along the river stretch promoted by sand abstraction.
- In the fall, P4 turned and fell upstream, which could only be possible if the paving stones were removed from the foundation base of the pillar by the infra-excavation resulting from scour.
- The riprap placed in P2 and P3 prevented these pillars from collapsing in the 2000–2001 floods and, probably, in other past and equally intense floods.
- The stability of the collapsed P4 could have been guaranteed if a protection solution identical to that found in P2 and P3 had been implemented.

The necessary lessons from the events that led to the Hintze Ribeiro Bridge collapse must be drawn from an in-depth analysis of the causes and consequences of this accident so that catastrophes like this one are not repeated in the future. It is important to emphasize the need to keep hydrographic surveys of riverbeds updated, which can only be done through constant monitoring and effective inspections. Particularly noteworthy is the need to implement restrictions on granting or renewing licenses for extracting sand from alluvial riverbeds. These should be granted only for short periods of time (having the hydrological year as a good reference) and only if certain conditions are met, including:

- i. Presentation of a sufficiently detailed topographic survey, covering the areas upstream and downstream of the sediment abstraction stretch and not just the affected area;
- ii. Verification that the current levels of the riverbed and that the extracted sand correspond to the values that were authorized;
- iii. With the new license, the maximum amounts of sand to be extracted must be fixed, together with the respective abstraction sites.

IntechOpen

IntechOpen

Author details

José Simão Antunes Do Carmo
FCTUC, Department of Civil Engineering, University of Coimbra, Coimbra,
Portugal

*Address all correspondence to: jsacarmo@dec.uc.pt

IntechOpen

© 2021 The Author(s). Licensee IntechOpen. This chapter is distributed under the terms of the Creative Commons Attribution License (<http://creativecommons.org/licenses/by/3.0>), which permits unrestricted use, distribution, and reproduction in any medium, provided the original work is properly cited. 

References

- [1] Sousa J.J., Bastos L., Multi-temporal SAR interferometry reveals acceleration of bridge sinking before collapse. *Natural Hazards and Earth System Sciences*. 2013;13(3):659–667. DOI: 10.5194/nhess-13-659-2013.
- [2] Pinto D.F., A Terceira Dimensão. Blogue in <http://portugalfotografiaaerea.blogspot.pt/2014/07/entre-os-rios.html> 2014 (Accessed October 30, 2020).
- [3] Rocha J.S., Antunes Do Carmo J.S., Lemos L.J.L., Silva V.D., Rebelo C.A.S., Bridges built on alluvial beds: The failure of the Hintze Ribeiro Bridge. *Recursos Hídricos*. 2008;29(2): 41–57 (*in Portuguese*).
- [4] Antunes Do Carmo J.S., Natural responses to changes in morphodynamic processes caused by human action in watercourses: A contribution to support management. *International Journal of Disaster Risk Reduction*. 2017;24:109–118. DOI:10.1016/j.ijdr.2017.05.014.
- [5] Teixeira P., A Ponte de Portugal. *Gaiense journal*. 2011 (*in Portuguese*).
- [6] Rocha J.S., Alves E., *Plano Específico Preliminar de Extracção de Inertes na Albufeira de Crestuma-Lever, Rio Douro*, LNEC - Laboratório Nacional de Engenharia Civil. 2002, Report 186/02-NHE, July (*in Portuguese*).
- [7] Araújo e Silva A.F., Ponte de Entre-os-Rios sobre o Rio Douro, Memória Descritiva. *Revista de Obras Públicas e Minas*, Tomo XIV. 1883:1–24 (*in Portuguese*).
- [8] Antunes Do Carmo J.S., Environmental impacts of human action in watercourses. *Natural Hazards and Earth System Sciences Discussions*. 2014; 14:1–32. DOI:10.5194/nhessd-14-1-2014.
- [9] MacCormack R.W., Numerical solution of the interaction of a shock wave with a laminar boundary layer. *Lecture Notes in Physics*. 1971;8:151–163.
- [10] Garcia R., Kahawita R.A., Numerical solution of the Saint-Venant equations with the MacCormack finite-difference scheme. *International Journal for Numerical Methods in Fluids*. 1986;6(5):259–274.
- [11] Antunes Do Carmo J.S., Seabra Santos F.J., Almeida A.B., Numerical solution of the generalized Serre equations with the MacCormack finite-difference scheme. *International Journal for Numerical Methods in Fluids*. 1993;16: 725–738. DOI: 10.1002/flid.1650160805.
- [12] Chiang Y.-C., Hsiao S.-S., Lin M.-C., Improved technique for controlling oscillation of coastal morphological modeling system. *Journal of Marine Science and Technology*. 2011;19(6): 625–633.